

**MEMORANDUM**

Date: November 6, 2002, Chandra Calibration Workshop  
 From: Eli Beckerman, Diab Jerius  
 Subject: Modelling Chandra: Positional Accuracy of Mirror and Detector Models  
 Version: 1.0

**Abstract**

Chandra users will soon have two ways of modelling sources observed with Chandra – MARX, and a new tool, ChaRT. ChaRT is a web front end to the official Chandra mirror model, *SAOsc*, which until now was not available for the end user. MARX also provides detector models. The CIAO tool *psf\_project\_ray*, which is designed to be used with the events generated by *SAOsc*, provides a model of the detector geometries. We present the first in a series of studies comparing the accuracy of the models. We focus here on the positional accuracy, that is, can the models correctly predict where a source will appear on a detector. We compare events generated by *SAOsc* and detected by MARX, *psf\_project\_ray*, and a third, engineering model, *deticpt*, as well as events generated by MARX and detected by MARX. We present results for various off-axis pointings of AR Lac, LMC-X1, HR1099, and PKS0637-752 on all of Chandra’s detectors.

**1 Introduction**

*SAOsc* is the suite of programs developed by the Chandra X-ray Center (CXC) Optics Group to provide a high-fidelity model for Chandra’s High Resolution Mirror Assembly (HRMA). This full raytrace simulation model has been used in the calibration of telescope performance, and the model has undergone revisions based on ground-calibration data taken at the X-ray Calibration Facility (XRCF) in Huntsville, AL, and on in-flight observations. With the upcoming release of the Chandra Ray Tracer (ChaRT), a web interface to *SAOsc*, users will have access to this detailed model of the HRMA.

MARX was developed by the MIT/CXC group to provide a detailed raytrace simulation of the on-board telescope performance, while maintaining a high degree of speed and portability. The MARX mirror model is essentially a simplified version of the *SAOsc* model. In addition to its model of the HRMA, MARX includes models of the Chandra gratings and detectors. The full MARX suite has been available to users to simulate on-orbit performance of Chandra and to aid in writing proposals. For fine details of the effects of the mirror structure on Chandra data, the *SAOsc* raytrace model is necessary.

*SAOsc* raytraces may be sent through the MARX detector and gratings models, and conversely, it is possible to send simulated MARX rays through *SAOsc*. In fact, there are a variety of combinations of mirror and detector models, and the number of options is growing. This report looks at the positional accuracy of the *SAOsc* raytraces through 3 different detector models: MARX (MIT), *psf\_project\_ray* (CIAO), and *deticpt* (CXC engineering model). In addition, we study full MARX simulations using both the mirror and detector models of the MARX software suite. We use on-orbit observations of bright point sources on every detector and at a variety of off-axis angles to probe the positional accuracy of the different simulation methods.

**2 Observation Summary**

We searched the Chandra Data Archive for every observation of the 4 bright point sources shown in the table below. We used only those observations with no *sim\_z* offset to ensure that the optical axis fell on the detector aimpoint. Raytracing any *sim\_z* offsets would have been too difficult for our purposes. Our sample is predominantly HRC calibration observations of AR Lac, which were taken as mini-scans to determine small-scale gain variations.

Detector	# LMC X-1	# HR 1099	# PKS0637-752	# Ar Lac	Total
ACIS-I	4	4	0	0	8
ACIS-S	20	0	19	0	39
HRC-I	6	17	0	139	162
HRC-S	19	0	0	84	103
Total	49	21	19	223	-

Table 1. Number of Observations of Each Source, On Each Detector

### 3 Centroiding the Data

To determine accurate detector positions from the point source observations, we used the DETX and DETY coordinates, which are not corrected by the aspect solution. To remove the telescope dither, we utilized a program named *deosc*, which removes time-dependent oscillations from an event list. *deosc* performs a fit to the time-varying position of the object’s center, and subtracts this fit from the data to provide corrected detector coordinates. After removing the telescope motion from the detector coordinates, we used a sigma clipping algorithm to find accurate centroids. Since *deosc* performs a similar sigma-clipping to the data before subtracting the motion, the source centroids are very close to those determined by *deosc*. Once these centroids were found, *dmcoords* was used to convert these positions into Mirror Spherical Coordinates (MSC) [1], or  $\theta$  and  $\phi$ . These coordinates were then used to raytrace these observations and check for coordinate system consistency.

### 4 Simulations

Using the MSC coordinates for each of the observations, we generated rays using *SAOsac* and MARX mirror models. The *SAOsac* rays were passed through to the 3 detector models detailed in this study, while the MARX rays were sent through the MARX detector model. The source spectrum for each object was incorporated into the raytrace, though the effect on the positional accuracy would have been minimal. Each raytrace typically has  $\sim 10,000$  detected photons. Once the observations were modelled, we were able to centroid the simulated data and compare detector positions to those measured from the observed images. Differences in positional centroids could lead to an understanding of systematic differences in the various raytrace and detector models.

Simulations were carried out using *SAOsac* with the `orbit_XRCF+tilts_04` configuration, MARX version 4.0, *deticpt* version D20011106, and *psf-project\_ray* version CIA0 2.2. All analysis corresponds to CALDB 2.17.

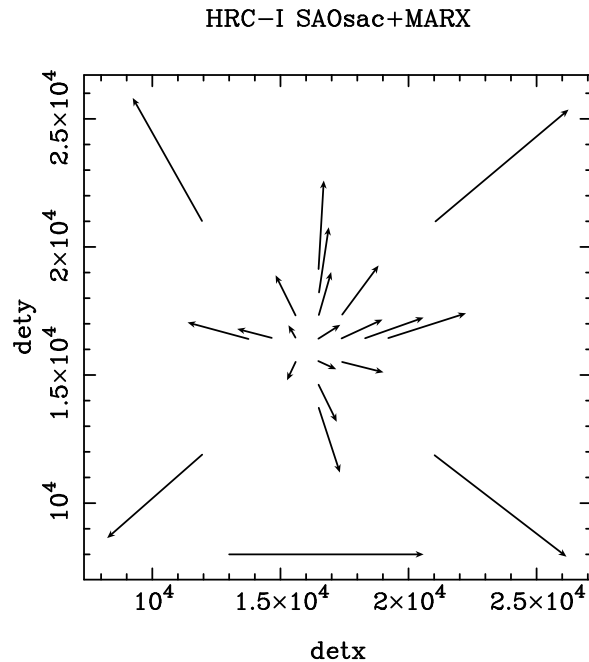


Figure 1: This set of AR Lac simulations shows a plate scale factor which turns out to be due to a  $\sim 9$ mm offset in the default value for the MARX focal length. The positional offsets were scaled by a factor of 1000 to better display the vector field. The horizontal arrow at the bottom represents 1" ( $\sim 7.5$  HRC pixels) in this scaling convention.

## 5 Analysis

Vector fields of the deviations from the centroided detector positions of the observations to the centroided detector positions of the simulations are shown in Figures 1, 2, 3, 4, and 5. Originally, we found the runs through *deti* and *psf-project-ray* matched pretty closely, while a linear stretch was evident in both MARX setups. This is demonstrated in Fig. 1, where the vector field points radially outward, and the deviations increase with off-axis distance. This turned out to be due to an offset of  $\sim 9$ mm in the default value for the MARX focal length. The remainder of the analysis shown here incorporates the focal length provided in the CALDB, and the obvious platescale effects disappear.

Figure 2 shows the simulations for the HRC-I observations. All 4 simulation realizations are compared, and the shifts from the observed DETX and DETY positions are magnified by a scale factor of 1000. The arrow at the bottom depicts  $1''$ , or  $\sim 7.5$  HRC pixels, using the same scaling factor.

Figures 3 and 4 show the simulated runs on the HRC-S array, with the latter providing a more detailed look at only the central plate of the S-array.

Figure 3 shows that there are some problems in positional accuracy on simulations for the outer plates. The HRC-S is made up of 3 flat elements, with the outer 2 tilted to approximate the Rowland circle of the LETG. Raytraces for the outer plates have significant ( $> 1''$ ) deviations. Simulations for the central plate are shown in more detail in Fig. 4. On the central plate, the raytrace simulations primarily exceed the accuracy of an HRC pixel ( $0.13175''$ ). *deti* produces remarkably accurate positions up to about  $5'$  off-axis. Further off-axis the deviations reach up to one HRC pixel. Both sets of simulations using MARX appear to have a distortion towards the upper right, which seem to scale with distance off-axis. In all simulations, observations with roughly the same detector coordinates are raytraced to fall in different directions from the original position.

Figure 5 displays the results of the simulations for ACIS-S, using 20 observations of LMC X-1 and 19 of PKS0637-752. PKS0637 was the original focus source for calibration of Chandra's focal position, and includes an X-ray jet. The jet doesn't appear to interfere with this study. We do not present results for ACIS-I, as there were only 8 observations on the I array, and half of those were problematic.

The results for ACIS-S are clearly not as good as simulations for the HRC. Figure 5 shows observations across several of the chips, and future work will look for systematic chip-to-chip effects. While *SAOsac* and *deti* appear to be very accurate in determining detector positions on-axis, simulations of the off-axis pointings result in deviations greater than  $1''$ . Curiously, the MARX runs have  $\sim 0.5''$  shifts on-axis, all in the same direction. Offsets from the observed centroids for off-axis pointings are greater for both the MARX raytrace and *SAOsac*+MARX combination than they are for *deti* and *psf-project-ray*.

## 6 Conclusion

The raytraces and detector models studied in this report demonstrate the internal consistencies of the coordinate system transformations, the accuracy of the *SAOsac* and MARX models of the optical bench, and the proper modelling of the location of photons hitting the detectors. Shifts in the centroids from the observed data to the simulated data do occur, and they increase with off-axis angle  $\theta$ .

Especially for on-axis pointings, the raytrace and detector models provide a very accurate reproduction of photons travelling through the telescope and hitting the detector. Probably due to similarities in their construction, the CIAO tool *psf-project-ray* and the engineering model *deti* have almost identical results, though there are clearly differences on HRC-S. The *SAOsac*/MARX combination and the full MARX raytrace have significant differences in the directionality of the offsets, and minor differences in amplitude. Problems in positional accuracy become more prominent for large off-axis pointings. Odd behavior of *psf-project-ray* on HRC-S manifests itself in consistent downward (to smaller DETY) shifts on the central plate, and this needs to be studied in better detail. It is also unclear at this point whether HRC-S simulations which were observed to have roughly the same detector coordinates were found to have larger offsets in the Mirror Spherical Coordinate system, or if the raytraces actually shifted them in different directions.

Currently, we are working to extend this study to extreme off-axis source detections using the database of cell-detect runs on all available Chandra data. This will provide a better idea of the limitations and successes of the various simulation methods. Additionally, any platescale problems or improper modelling of the tilt of the S arrays will be more apparent.

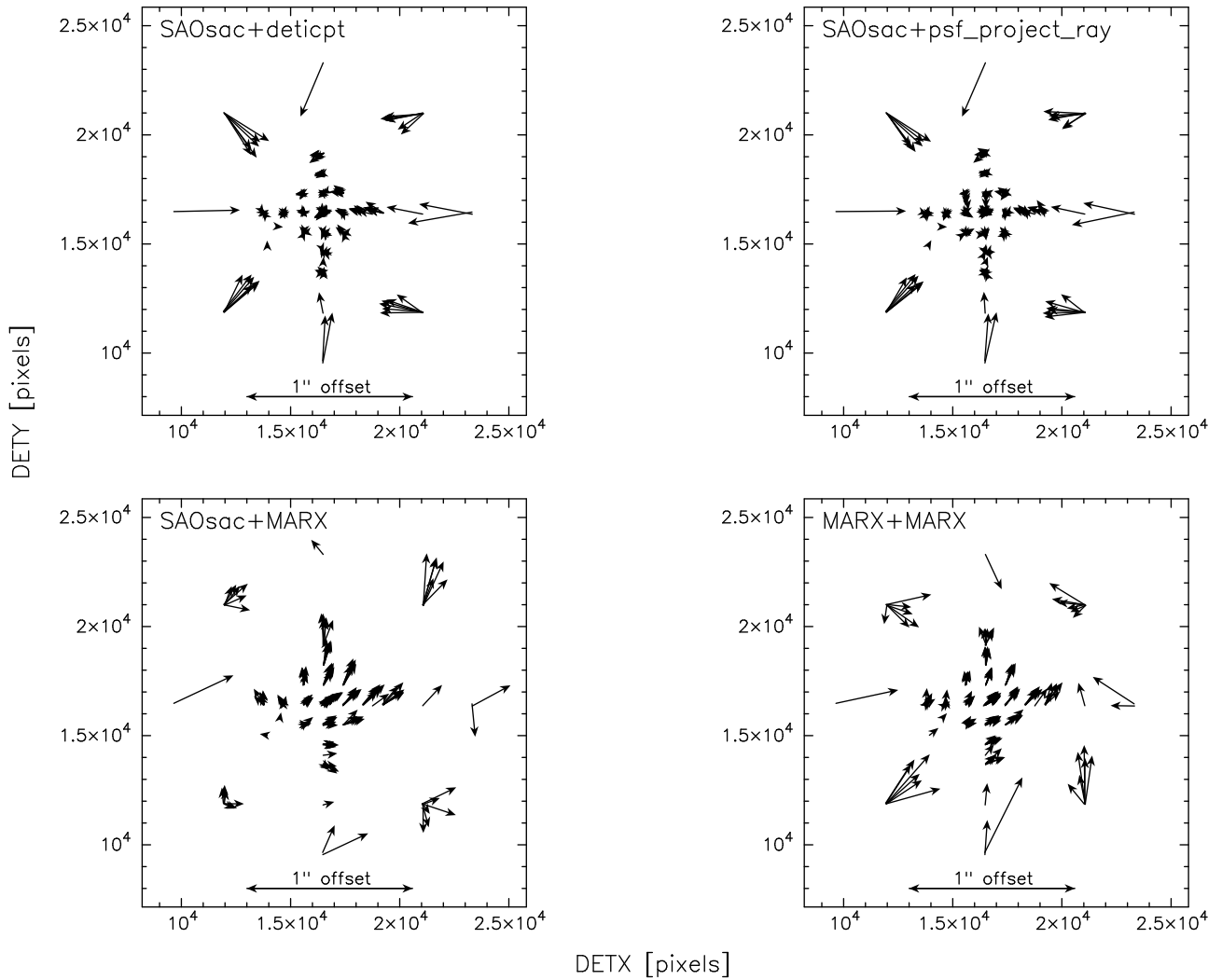


Figure 2: Comparisons of the 4 experimental setups is shown here for the HRC-I. Arrows represent the shift from centroids of the observed detections to centroids of the simulated rays, with the arrow lengths scaled by a factor of 1000 to exaggerate the deviations. The arrow at the bottom denotes  $1''$  ( $\sim 7.5$  HRC pixels) in this scaling convention. As the HRC-I is a flat plate  $\perp$  to the optical axis, the deviation from the focal surface increases as a source moves off-axis. Discrepancies from the observations might appear because of detector models inadequately taking this into account. The directionality of the vector field as well as apparent linear scaling with distance indicates that this might be a plate scale effect, with a magnitude of  $\sim 0.02\%$ .

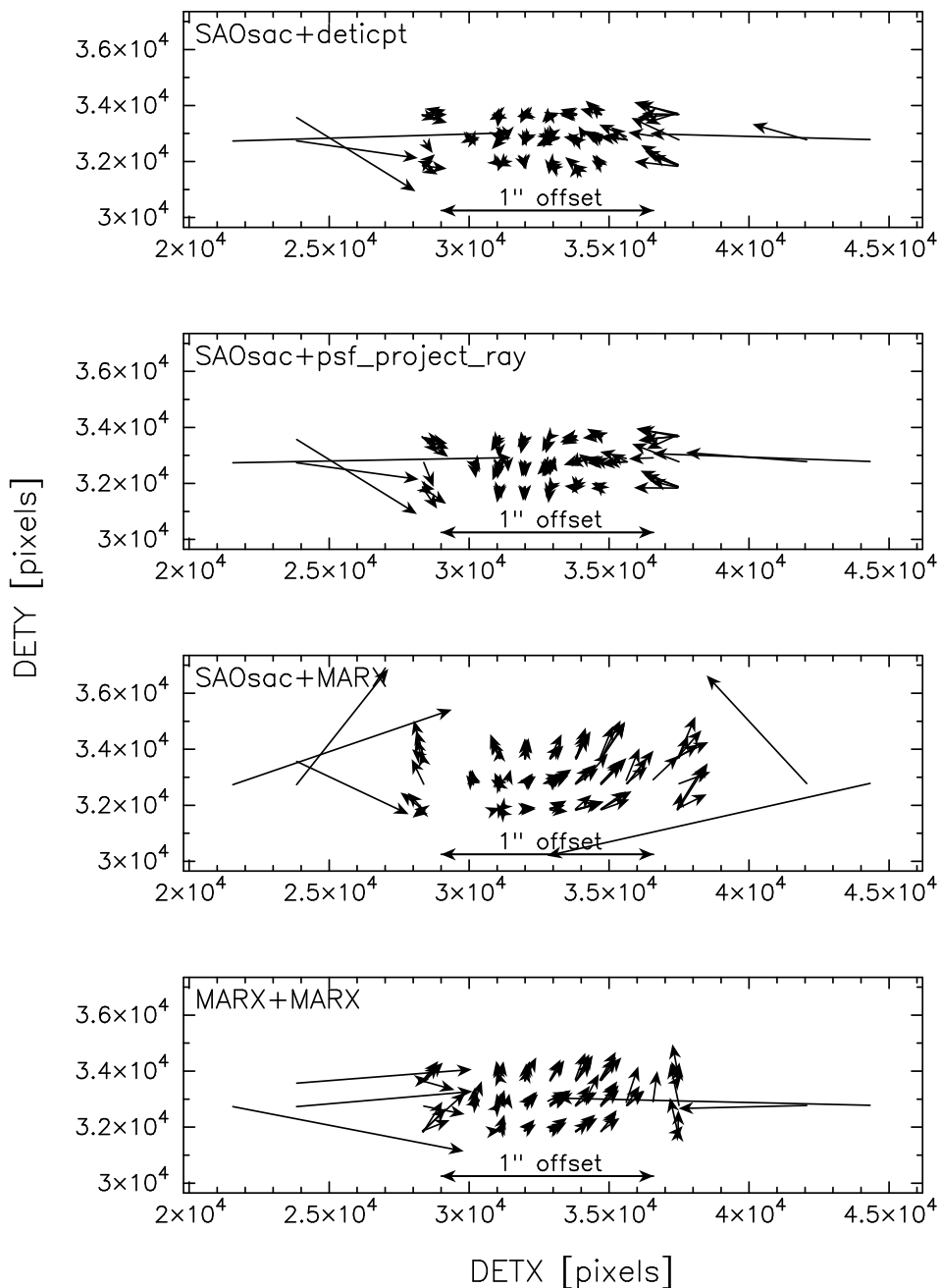


Figure 3: An overview of the simulated observations on the HRC-S. Arrows represent the shift from centroids of the observed detections to centroids of the simulated rays, with the arrow lengths scaled by a factor of 1000 to exaggerate the deviations. The arrow at the bottom denotes  $1''$  ( $\sim 7.5$  HRC pixels) in this scaling convention. The HRC-S is made up of 3 flat elements, with the outer 2 tilted to approximate the Rowland circle of the LETG. Raytraces for the outer plates have significant ( $> 1''$ ) deviations. The simulations for the central plate are shown in more detail in Fig 4

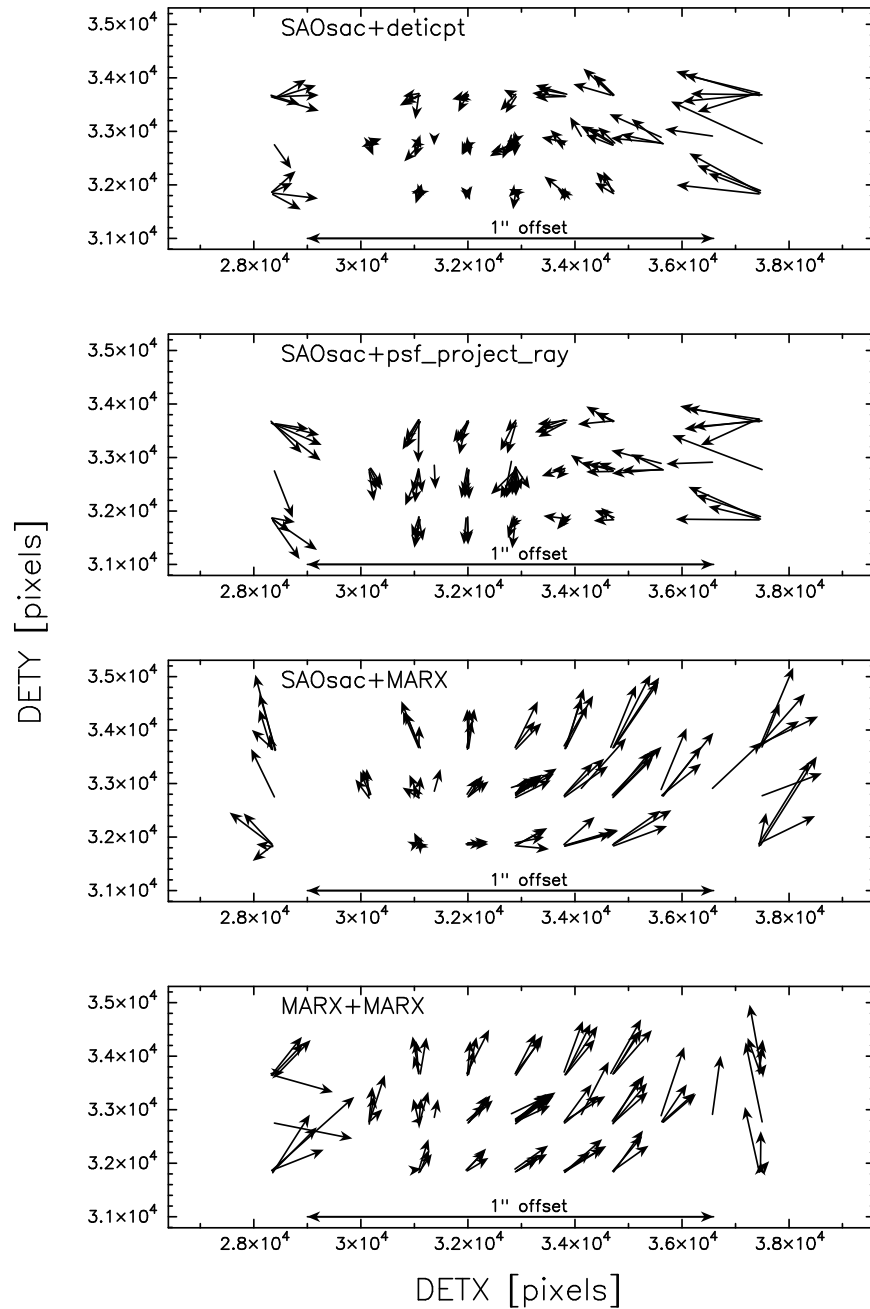


Figure 4: A closer look at the central plate of the HRC-S. On the central plate, the raytrace simulations primarily exceed the accuracy of an HRC pixel ( $0.13175''$ ). *deticpt* produces remarkably accurate positions up to about  $5'$  off-axis. Further off-axis the deviations reach up to one HRC pixel. Both sets of simulations using MARX appear to have a distortion towards the upper right, which seems to scale with distance off-axis. Arrow lengths are scaled by a factor of 1000 to exaggerate the deviations. The arrow at the bottom depicts  $1''$  ( $\sim 7.5$  HRC pixels) in this scaling convention.

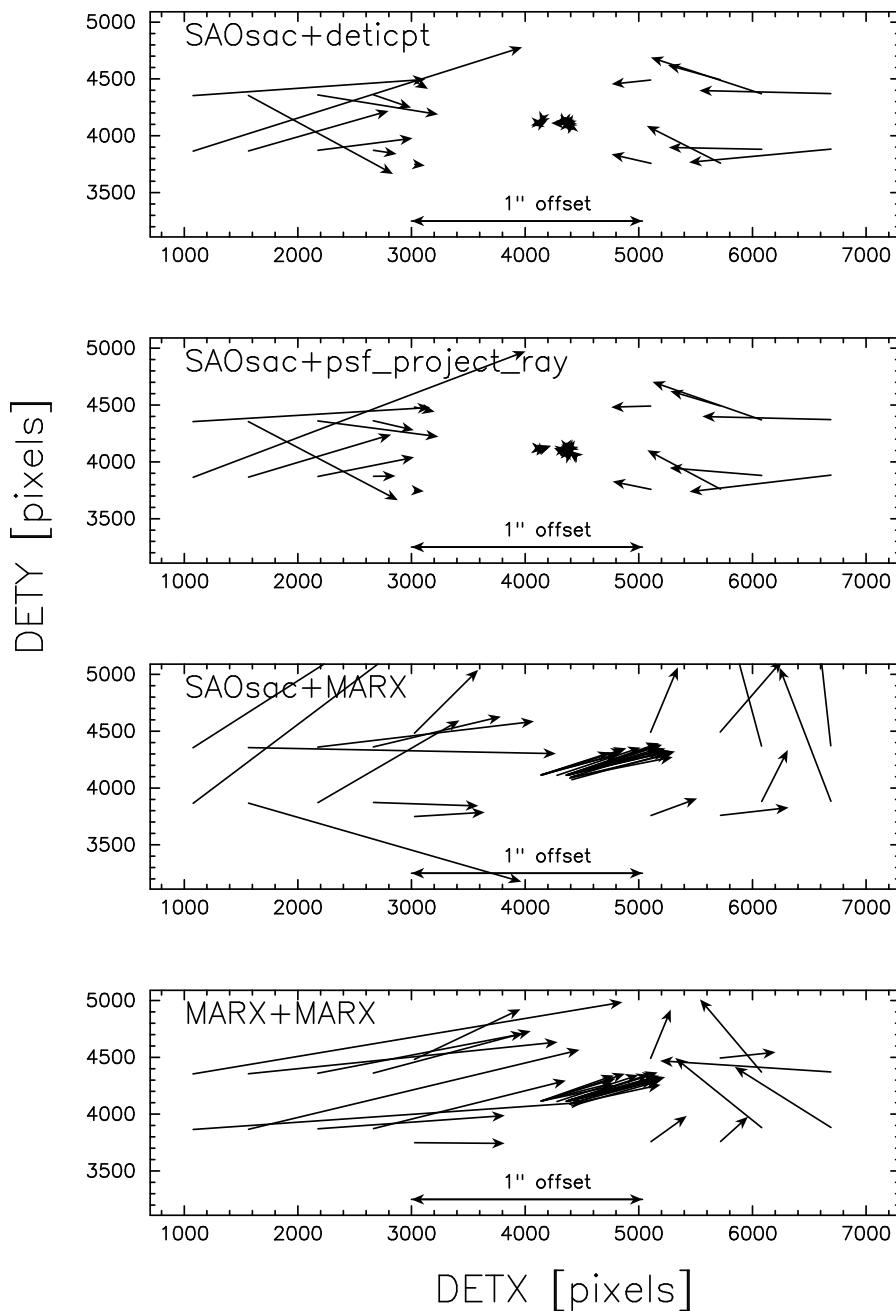


Figure 5: These simulations of ACIS-S observations are comprised of roughly half LMC X-1 and half PKS0637-752 pointings. The arrow at the bottom indicates an arrow-length of 1". Positional shifts of greater than 1" are abundant. The ACIS-S chips are tilted to approximate the shape of the HETG Rowland circle, and thus deviate from the focal surface of the HRMA. Additionally, the ACIS-S array extends to significant off-axis angles, where the HRMA PSF will be broader.

## References

- [1] J. McDowell, Coordinate Systems: Paper I, 2001 May 13  
(<http://cxc.harvard.edu/contrib/jcm/ncoords.ps>)